ChemPubSoc Europe

DOI: 10.1002/chem.201705609

CHEMISTRY
A European Journal
Full Paper

Crystal Engineering |Hot Paper|

Formation of Water Channels in the Crystalline Hydrates of Macrocyclic Compounds

Rahul S. Patil, Chen Zhang, Kanishka Sikligar, Gary A. Baker, and Jerry L. Atwood*[a]

Abstract: Crystalline hydrates of macrocyclic compounds such as pyroagllol[4]arenes (PgCs) and resorcin[4]arenes (RsCs) are rare owing to their lower water solubility. Functionalization of these macrocyclic compounds is an affordable way to enhance water solubility. However, functionalization also encounters the formation of multiple conformers and subsequent difficulty in purification of the product. Herein, four novel crystalline hydrates of functionalized PgCs and RsCs were synthesized. Formation of water channels and the effects of intermolecular interactions on the physical properties of these novel hydrates are discussed.

Introduction

Unique cyclic shape and ability to carry different functional groups make macrocyclic compounds eligible for applications in the fields such as pharmaceuticals,[1,2] chromatography,[3,4] nanotechnology,[5,6] and gas sorption/separation.[7,8] For example, cyclodextrin, a cyclic oligomer of glucose has proven to be useful in pharmaceutical product development owing to higher water solubility and ability to form stable inclusion complex with drug molecules.[9] Higher crystallinity and ease of the synthesis are major advantages of these macrocyclic compounds for respective applications. The list of such macrocyclic compounds includes calixarenes, cucirbiturils, pillarenes, and cyclodextrins. Similar to cyclodextrin, pyrogallol[4]arenes (PgCs) and resorcin[4]arenes (RsCs), subclasses of calix[4]arenes often exhibit a unique bowl-like shape with hydroxy functional groups.[10–12] An upper rim of a typical RsC/PgC bowl consists of eight or 12 hydroxy groups while the lower rim consists of *C*-alkyl tails arising from the bridging methine group connecting two pyrogallol/resorcinol moieties (Figure 1). The presence of hydroxy groups make the upper rim of RsC/PgC more hydrophilic whereas *C*-alkyl groups make the lower rim more hydrophobic in nature.[13,14] Thus, crystal structures of RsC and PgC show unique architectural arrangements such as bilayer, capsular, or tubular geometries.[15–17] In particular, capsular arrangement of RsCs and PgCs includes hydrogen-bonded hexamers, metal coordinated hexamers, and dimeric skewed capsules in a given crystallizing medium.[16,18–22] Although multiple crystalline forms, solvates, and cocrystals of RsCs and PgCs are reported, hydrates of RsC and PgCs are uncommon.[23–27] Lower water solubility is one of the major causes of difficulty in the crystallization of the hydrates of RsCs and PgCs. Applications of RsCs and PgCs in pharmaceutical product development and biological systems are also limited as a result of low water solubility and subsequent poor bioavailability.[28] Water solubility of RsCs has been improved with functionalization of the upper rim with methylsulfonato groups.[29–31] However the presence of bulky sulfonato groups hinders the interaction of guest molecules with upper-rim hydroxy groups. Another approach to improve water solubility is functionalization at the lower *C*-alkyl tail or at the bridged methine group of RsC/PgC.[32,33] Pre-

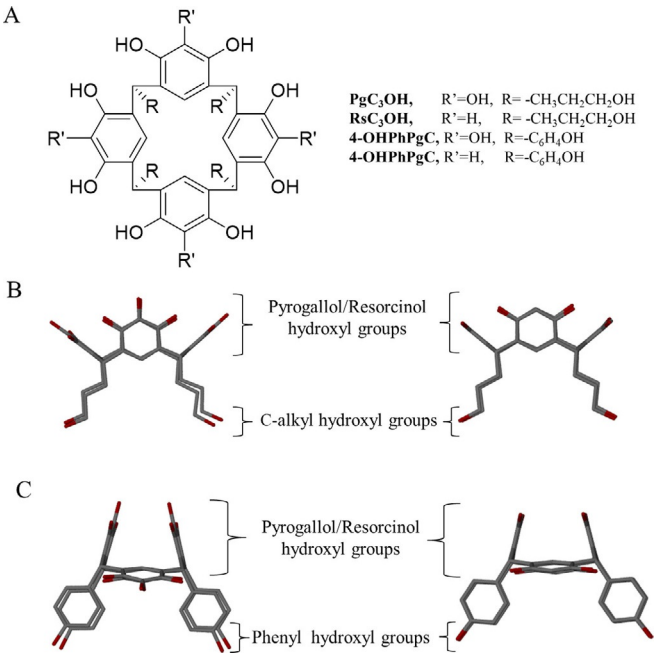


Figure 1. A) Representation of macrocyclic compounds. B) Pyrogallol/resorcinol and *C*-alkyl hydroxy groups in PgC_3OH and RsC_3OH. C) Pyrogallol/resorcinol and phenyl hydroxy groups in 4-OHPhPgC and 4-OhPhRsC. Gray = carbon, red = oxygen, hydrogen atoms are removed for clarity.

[a] R. S. Patil, C. Zhang, K. Sikligar, G. A. Baker, J. L. Atwood
Department of Chemistry, University of Missouri, 601 S. College Ave., Columbia, MO 65211 (USA)
E-mail: atwoodj@missouri.edu

Supporting information and the ORCID identification numbers for the authors of this article can be found under https://doi.org/10.1002/chem.201705609.

© 2018 Wiley-VCH Verlag GmbH & Co. KGaA, Weinheim

vious studies also demonstrated the formation of cogged hexameric nanotubular architecture from PgCs with unique branched alkyl tails.[15,34] However, functionalization at the bridged methine group, especially phenyl functionalization, may be associated with the formation of a mixture of conformers such as cone, boat, chair, saddle, and diamond.[35,36] Separation of major conformers has been achieved with solvent extraction methods.[32] Functionalization of the lower rim of RsC/PgC thus produces distinct framework architecture in the crystalline state as well as multiple conformers.[37] Therefore, to expand the range of tail functionalized RsCs and PgCs, we synthesized crystalline hydrates of *C*-propyl-3-ol-resorcin[4]arene (RsC_3OH), *C*-propyl-3-ol-pyrogallol[4]arene (PgC_3OH), 4-hydroxyphenylresorcin[4]arene (4-OHPhRsC), and 4-hydroxyphenylresorcin[4]arene (4-OHPhPgC) (Figure 1 A). These novel hydrates have now been characterized by single-crystal X-ray diffraction (SCXRD). Physical properties such as structural uniformity, thermal degradation/stability, and phase transformation of these crystalline hydrates of RsC and PgC have been evaluated with differential scanning calorimetry (DSC), thermogravimetric analysis (TGA), coupled with ^{1}H nuclear magnetic resonance (NMR) spectroscopy and powder X-ray diffraction (PXRD).

Materials and methods

An acid-catalyzed condensation reaction is used for the synthesis of PgC_3OH and RsC_3OH, from resorcinol/pyrogallol and 2,3-dihydrofuran with high purity and yield (Figures S1 and S2 in the Supporting Information).[33] Similarly 4-OHPhPgC and 4-OHPhRsC are synthesized from resorcinol/pyrogallol and 4-hydroxybenzaldehyde in the presence of concentrated hydrochloric acid at reflux temperature.[35] The crude product of the synthesis of 4-OHPhPgC and 4-OHPhRsC contains mixture of two major conformers such as chair and cone/boat. Thus, the separation of conformer is carried out with the previously reported solvent extraction method.[32] This purification and separation method produces the boat/cone conformer of 4-OHPhPgC and 4-OHPhRsC with high purity (Figures S3 and S4). Crude products of PgC_3OH, RsC_3OH, boat conformers of 4-OHPhPgC, and boat conformer of 4-OHPhRsC are heated in deionized water at 80 °C to obtain a clear solution. Gradual cooling of the clear solutions to room temperature yielded single crystals suitable for SCXRD data collection. SCXRD data was then reduced and refined to obtain crystal structures of the respective hydrates. The bulk crystalline hydrates were synthesized by scaling up the respective single crystal growth experiments. These bulk crystalline hydrates were then used for evaluation of physical properties such as bulk crystallinity, thermal stability, and structural uniformity.

Results and Discussion

The crystal structure of **1** [$(PgC_3OH)\cdot3(H_2O)$] consists of cone-shaped PgC_3OH with intramolecular O–H···O (2.69–2.85 Å) hydrogen bonds among the eight hydroxy groups of the upper rim of PgC_3OH. These intramolecular hydrogen-bonding interactions are responsible for maintaining the cone shape of PgC_3OH with C_{2v} symmetry (Figure S5). Pyrogallol hydroxy groups of the parent PgC_3OH form four O–H···O (2.74–2.85 Å) hydrogen bonds with pyrogallol hydroxy groups of PgC_3OH arranged head-to-head with respect to a parent PgC_3OH (Figure 2 A). The parent PgC_3OH also forms three O–H···O (2.67–2.78 Å) hydrogen bonds with *C*-alkyl hydroxy groups of two neighboring PgC_3OH molecules situated on either side of the parent PgC_3OH(Figure 2 A). Two pyrogallol hydroxy groups of the parent PgC_3OH interact with *C*-alkyl hydroxy groups of PgC_3OH situated above with respect to the parent PgC_3OH through O–H···O (2.68–2.80 Å) hydrogen bonds. (Figure 2 A) A pyrogallol hydroxy group of the parent PgC_3OH also forms an O–H···O (2.75 Å) hydrogen-bonding interaction with a water molecule situated above the respective pyrogallol hydroxy group (Figure 2 A). Thus, the pyrogallol hydroxy groups of the parent PgC_3OH interact with one water molecule and four neighboring PgC_3OH molecules through O–H···O hydrogen-bonding interactions. Similarly, *C*-alkyl hydroxy groups form O–H···O (2.75–3.08 Å) hydrogen bonds with two water molecules

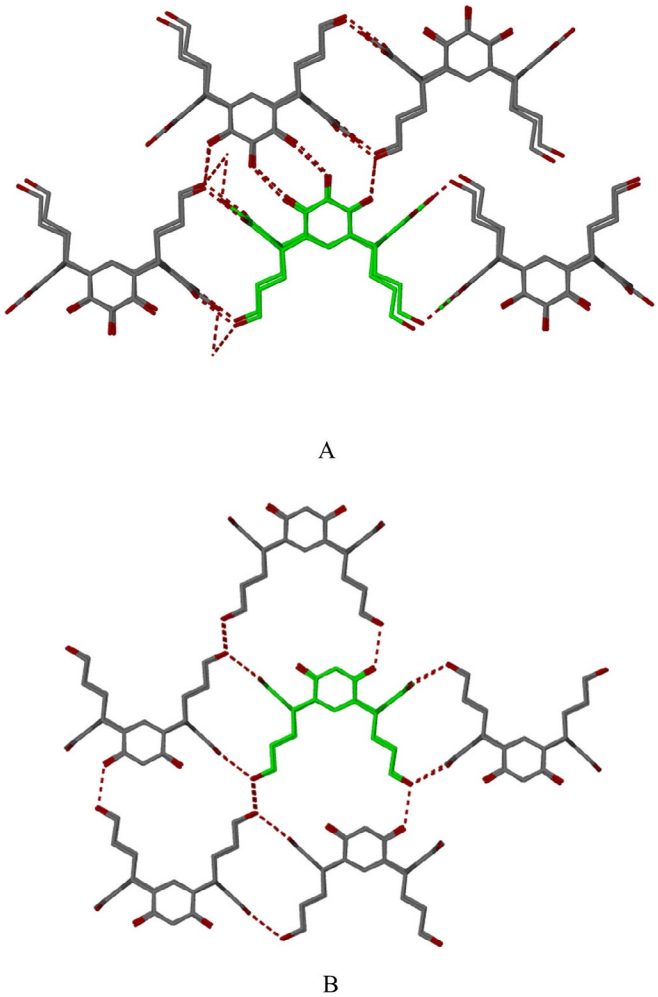


Figure 2. A) Intermolecular hydrogen-bonding interactions between parent PgC_3OH and neighboring PgC_3OH molecules and the water molecule in **1**. B) Intermolecular hydrogen-bonding interactions between parent RsC_3OH and neighboring RsC_3OH in **2**. Color codes: Green (in parent PgC_3OH, RsC_3OH) or gray = C, red = O, hydrogen atoms are omitted for clarity.

© 2018 Wiley-VCH Verlag GmbH & Co. KGaA, Weinheim

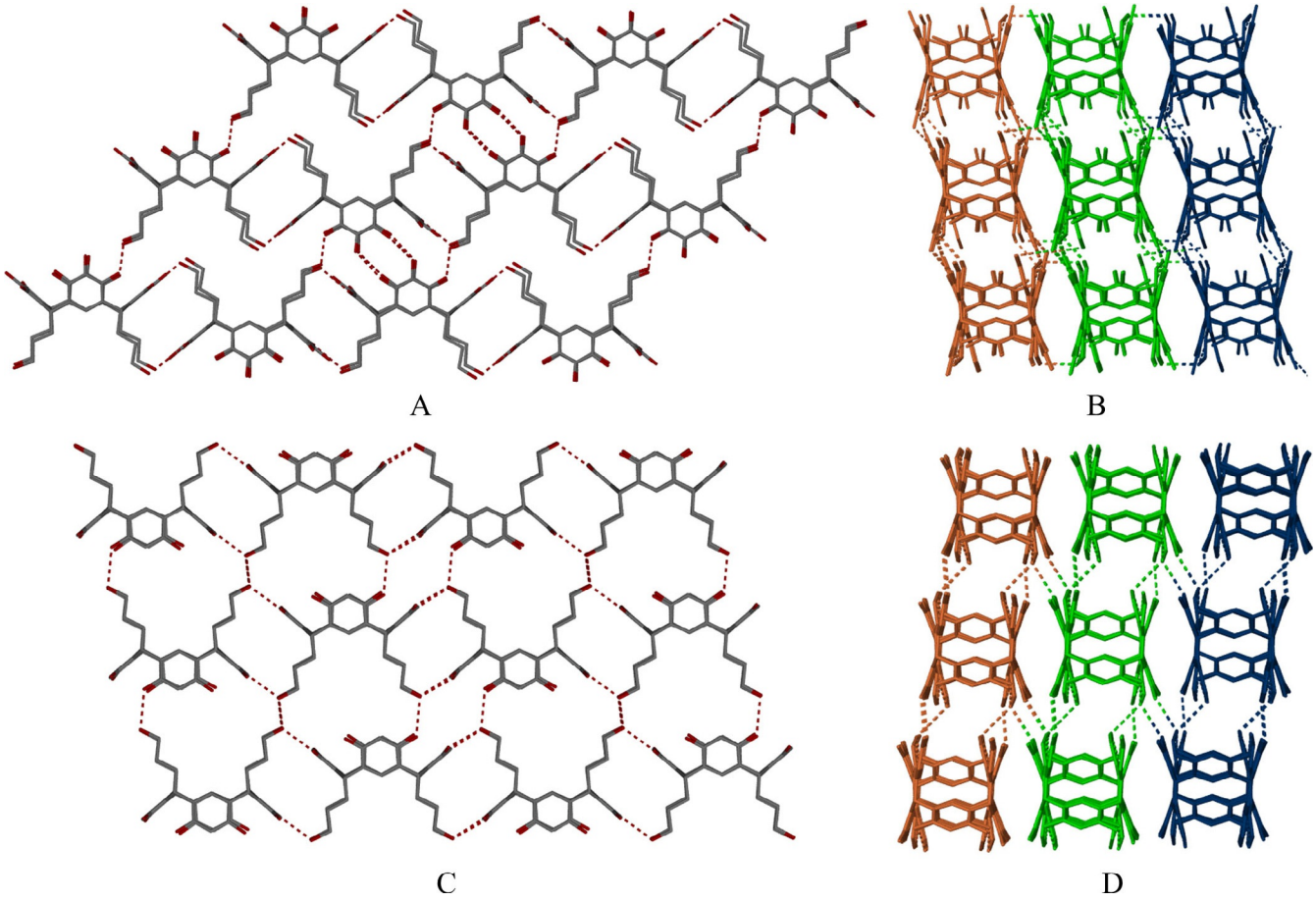


Figure 3. A) 2D Arrangement of hydrogen-bonded PgC_3OH molecules in the crystal structure of **1**. B) Hydrogen-bonding interactions between successive 2D planes of PgC_3OH molecules in the crystal structure of **1**. C) Formation of 2D architecture of hydrogen-bonded RsC_3OH molecules in the crystal structure of **2**. D) Hydrogen-bonding interactions between successive 2D planes of PgC_3OH molecules in the crystal structure of **2**. For (A) and (C): gray = C, red = O, hydrogen atoms are omitted for clarity.

on either side of the parent PgC_3OH (Figure 2A). *C*-alkyl hydroxy groups also form O–H···O hydrogen bonds with pyrogallol hydroxy groups of two neighboring PgC_3OH molecules on either side of the parent PgC_3OH (Figure 2A). These interactions strengthen the intermolecular interactions between the neighboring PgC_3OH and also result in the formation of a 2D hydrogen-bonded plane of PgC_3OH (Figure 3A). Two such parallel planes are connected through hydrogen-bonding interactions since the *C*-alkyl tail hydroxy groups of each PgC_3OH form O–H···O hydrogen bonds with the *C*-alkyl tail hydroxy groups of the PgC_3OH molecules situated in the neighboring parallel 2D plane (Figure 3B and Figure S7). These interactions thus result in the formation of the 3D framework in the extended crystal structure (Figure 3B). Two water molecules occupy the space in the bowl-shaped cavity of the PgC_3OH, and also form a mutual hydrogen bond. Thus, the extended crystal structure of **1** reveals the formation of water channels along the [11$\bar{1}$] crystallographic direction (Figure 4A).

The crystal structure of **2** [$(RsC_3OH)\cdot3(H_2O)$] consists of RsC_3OH in a cone conformation with C_{2v} symmetry. The cone shape of RsC_3OH is maintained by four O–H···O (2.72–2.80 Å) intramolecular hydrogen bonds among the eight resorcinol hydroxy groups of RsC_3OH (Figure S6). Similar to **1**, resorcinol hydroxy groups of the parent RsC_3OH in **2** form O–H···O (2.58–2.71 Å) hydrogen bonds with *C*-alkyl hydroxy groups of two neighboring RsC_3OH molecules situated on either side of a parent RsC_3OH (Figure 2B) .Resorcinol hydroxy groups also form O–H···O (2.76Å–2.81 Å) hydrogen-bonding interactions with *C*-alkyl hydroxy groups of RsC_3OH placed above with respect to the parent RsC_3OH (Figure 2B). *C*-alkyl hydroxy groups of the parent RsC_3OH form O–H···O (2.58–2.71 Å) hydrogen bonds with resorcinol hydroxy groups of two neighboring RsC_3OH on either side (Figure 2B). Similar O–H···O hydrogen-bonding interactions between *C*-alkyl hydroxy groups of the parent RsC_3OH and resorcinol hydroxy groups of RsC_3OH arranged tail-to-head with respect to the parent RsC_3OH (Figure 2B). These intermolecular interactions among RsC_3OH result in the formation of 2D planes of hydrogen-bonded RsC_3OH (Figure 3C). Additional O–H···O (2.76 Å) intermolecular interactions between *C*-alkyl hydroxy groups and resorcinol hydroxy groups connect two parallel 2D planes of RsC_3OH (Figure 3D). Resorcinol hydroxy groups and *C*-alkyl hydroxy groups also form O–H···O (2.82 and 2.66 Å, respectively) hydrogen bonds with one water molecule each (Figure S8). Three water

© 2018 Wiley-VCH Verlag GmbH & Co. KGaA, Weinheim

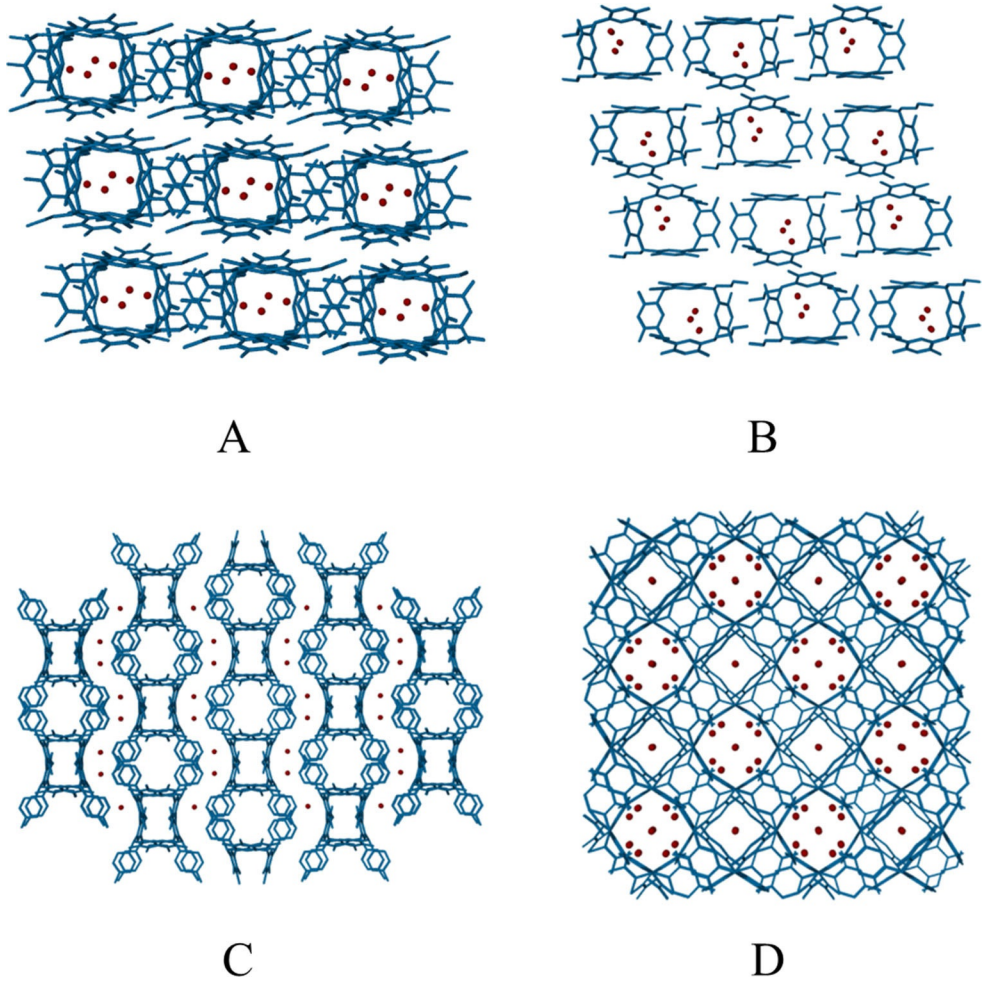


Figure 4. A) Formation of water channels along the [11$\bar{1}$] crystallographic direction in the crystal structure of **1**. B) Formation of water channels along the [100] crystallographic direction in the crystal structure of **2**. C) Water channel formed between two successive 2D layers of 4-OHPHPgC molecules in the crystal structure of **3**. D) Formation of water channels along the [001] crystallographic direction in the crystal structure of **4**. Blue = macrocycles, red = water, hydrogen atoms are omitted for clarity.

molecules occupy the space between two RsC_3OH molecules arranged head-to-tail, thus resulting in the formation of a water channel along the [100] crystallographic direction (Figure 4B).

The crystal structure of **3** [(4-OHPhPgC)·2(H_2O)] contains 4-OHPhPgC in the boat conformation with *rccc* orientation of the 4-hydroxyphenyl tails. Thus, there are no intramolecular hydrogen-bonding interactions between the pyrogallol hydroxy groups of 4-OHPhPgC. Pyrogallol hydroxy groups of a parent 4-OHPhPgC form O–H···O (2.86–2.97 Å) hydrogen bonds with the pyrogallol hydroxy groups of 4-OHPhPgC molecules arranged head-to-tail on either side of the parent 4-OHPhPgC (Figure 5A). Pyrogallol hydroxy groups also form four O–H···O (2.78 Å) hydrogen bonds with the pyrogallol hydroxy groups of two neighboring 4-OHPhPgC molecules placed on two opposite sides of the parent 4-OHPhPgC (Figure 5A). Two phenyl hydroxy groups also form O–H···O (2.78 Å) hydrogen bonds with two pyroagllol hydroxy groups of tail-to-tail-oriented 4-OHPhPgC molecules on each side of the parent 4-OHPhPgC (Figure 5A). Thus, the parent 4-OHPhPgC molecule interacts with six neighboring 4-OHPhPgC molecules through O–H···O hydrogen bonds. These intermolecular hydrogen bonds among 4-OHPhPgC molecules produce a 2D plane of 4-OHPhPgC molecules in the crystal structure (Figure S9). Two pyrogallol hydroxy and two phenyl hydroxy groups form O–H···O (2.68–2.74 Å) hydrogen bonds with six water molecules on the diagonally opposite sides with respect to each other (Figure S10). These water molecules occupy the space between two consecutive 2D planes of hydrogen-bonded 4-OHPhPgC molecules and resulted in the formation of water channels along the [001] crystallographic direction (Figure 4C).

The crystal structure of **4** [(4-OHPhRsC)·6(H_2O)] consists of 4-OHPhRsC in a boat conformation with four 4-hydroxyphenyl rings oriented *rccc* with respect to the axial and equatorial resorcinol components. All eight resorcinol hydroxy groups of a parent 4-OHPhRsC molecule form O-H···O (2.72 Å) hydrogen bonds with resorcinol hydroxy groups of two neighboring 4-OHPhRsC molecules situated on opposite sides of the parent 4-OHPhRsC molecule (Figure 5B). Four resorcinol hydroxy groups and four phenyl hydroxy groups form O–H···O (2.68–2.74 Å) hydrogen bonds with eight water molecules, four on each side of the parent 4-OHPhRsC (Figure 5B and Figure S10).

© 2018 Wiley-VCH Verlag GmbH & Co. KGaA, Weinheim

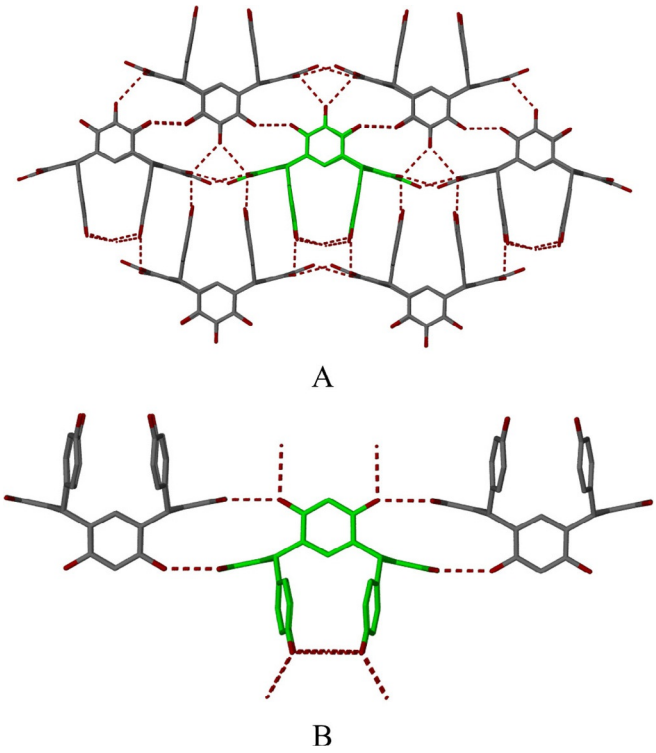


Figure 5. A) Hydrogen-bonding interactions between parent 4-OHPhPgC and neighboring 4-OHPhPgC molecules in **3**. B) Intermolecular hydrogen-bonding interactions between parent 4-OHPhPgC and neighboring 4-OHPHPgC molecules in **4**. Green (in parent 4-OHPhPgC and 4-OHPHRSC) or gray = C; red = O, hydrogen atoms are omitted for clarity.

Two water molecules also form O–H···O (2.94 Å) hydrogen bonds with two phenyl hydroxy groups. Thus one 4-OHPhRsC molecule interacts with ten water molecules. These water molecules occupy the space between the channel formed along the [001] crystallographic direction in the crystal structure (Figure 4D).

Formation of the water channels in the extended crystal structures of all the above-mentioned hydrates clearly initiates the bulk crystallization of these hydrates. The bulk crystalline materials **B1**, **B2**, **B3**, and **B4** were synthesized by scaling up the respective procedure of synthesis of hydrates **1**, **2**, **3**, and **4**. Uniformity of the bulk crystalline materials and phase similarity with the respective single crystal structures were confirmed with PXRD analysis. PXRD patterns of **B1**, **B2**, **B3**, and **B4** match well with the simulated PXRD patterns calculated from the single-crystal structures of **1**, **2**, **3**, and **4,** respectively (Figures S11–S14). TGA of **B1**, **B2**, **B3**, and **B4** reveals the loss of water solvent over the range of 100–150 °C and the complete degradation of dry solid at around 250 °C (Figures S15–S18). The effect of loss of water on the crystallinity of the bulk materials was also tracked with PXRD and measurement of water content by the Karl Fischer method. The comparison of the simulated PXRD patterns of **1**, **2**, **3**, and **4** with the respective PXRD patterns of **B1**, **B2**, **B3**, and **B4** after heating to 150 and 200 °C shows no loss of crystallinity (Figures S11–S14). Positions of peaks in the PXRD of **B1**, **B2**, **B3**, and **B4** after heating at 150 and 200 °C remain the same when compared to simulated PXRD of **1**, **2**, **3**, and **4,** respectively. However, the change in height and width of these peaks reflects a loss in crystallinity with the loss of water components from the bulk materials without breaking down the overall framework architecture. Thus, the loss of water in the crystalline bulk materials is attributed primarily to the partial removal of water from the framework. The DSC patterns confirm the subsequent rearrangement in the crystalline phase of bulk materials under ramping heat over the temperature range of room temperature to 450 °C (Figures S15–S18). A sharp endothermic peak in the DSC pattern of **B1** and **B2** reveals the melting of **B1** and **B2** in the broader range of 290–320 °C. Comparatively broader endothermic peaks in the DSC patterns of **B3** and **B4** confirm the complete degradation over the temperature range of 300–400 °C (Figures S17 and S18). These thermophysical characterization studies support the higher thermal stability and crystallinity of hydrates at the elevated temperature of 200 °C.

Conclusions

Properties of crystalline hydrates of PgC_3OH, RsC_3OH, 4-OHPhPgC, and 4-OHPhRsC are discussed herein. All four hydrates form a 3D arrangement of macrocycles supported with O–H···O hydrogen bonds between the hydroxy groups of macrocycles, which are often bridged by water molecules. Hydrogen-bonded water molecules exhibit formation of water channels along a particular crystallographic axis in the crystal structures. Although removal of all water molecules from these channels is prevented by the hydrogen-bonding interactions, TGA coupled with DSC and PXRD studies reveal the stability of these hydrates up to 200 °C. Thus, this article encourages potential applications of hydrates of macrocyclic compounds in pharmaceutical and material sciences.

Crystallographic information

CCDC 1587359 (**1**), 1587361 (**2**), 1587360 (**3**), 1587362 (**4**) contain the supplementary crystallographic data for this paper. These data are provided free of charge by The Cambridge Crystallographic Data Centre.

Conflict of interest

The authors declare no conflict of interest.

Keywords: crystal structures · macrocycles · hydrogen bonds · water channels

[1] A. Whitty, L. A. Viarengo, M. Zhong, *Org. Biomol. Chem.* **2017**, *15*, 7729.
[2] X. Ma, Y. Zhao, *Chem. Rev.* **2015**, *115*, 7794.
[3] B. Mokhtari, K. Pourabdollah, N. Dalali, *Chromatographia* **2011**, *73*, 829.
[4] G. Delahousse, R. Lavendomme, I. Jabin, V. Agasse, P. Cardinael, *Current Organic Chemistry* **2015**, *19*, 2237.
[5] A. R. Kongor, V. A. Mehta, K. M. Modi, M. K. Panchal, S. A. Dey, U. S. Panchal, V. K. Jain, *Topics in Current Chem.* **2016**, *374*, 1.
[6] Y. Tauran, B. Kim, A. W. Coleman, *J. Nanosci. Nanotechnol.* **2015**, *15*, 6308.

© 2018 Wiley-VCH Verlag GmbH & Co. KGaA, Weinheim

[7] R. S. Patil, D. Banerjee, C. M. Simon, J. L. Atwood, P. K. Thallapally, *Chem. Eur. J.* **2016**, *22*, 12618.
[8] R. S. Patil, D. Banerjee, C. Zhang, P. K. Thallapally, J. L. Atwood, *Angew. Chem. Int. Ed.* **2016**, *55*, 4523; *Angew. Chem.* **2016**, *128*, 4599.
[9] M. E. Davis, M. E. Brewster, *Nat. Rev. Drug Discovery* **2004**, *3*, 1023.
[10] K. N. Rose, L. J. Barbour, G. W. Orr, J. L. Atwood, *Chem. Commun.* **1998**, 407.
[11] L. R. Macgillivray, J. L. Atwood, *NATO Science Series, Series C: Mathematical and Physical Sciences* **1999**, *538*, 407.
[12] J. W. Steed, J. L. Atwood *Supramolecular Chemistry, Second edition*, John Wiley & Sons, Ltd.: United Kingdom **2009**.
[13] R. S. Patil, A. V. Mossine, H. Kumari, C. L. Barnes, J. L. Atwood, *Cryst. Growth Des.* **2014**, *14*, 5212.
[14] R. S. Patil, H. Kumari, C. L. Barnes, J. L. Atwood, *Chem. Commun.* **2015**, *51*, 2304.
[15] O. V. Kulikov, M. M. Daschbach, C. R. Yamnitz, N. Rath, G. W. Gokel, *Chem. Commun.* **2009**, 7497.
[16] L. R. MacGillivray, J. L. Atwood, *Nature* **1997**, *389*, 469.
[17] C. Zhang, K. Sikligar, R. S. Patil, C. L. Barnes, S. J. Teat, J. L. Atwood, *Chem. Commun.* **2017**, *53*, 9613.
[18] J. Dalgarno Scott, B. Bassil Daniel, A. Tucker Sheryl, J. L. Atwood, *Angew. Chem. Int. Ed.* **2006**, *45*, 7019; *Angew. Chem.* **2006**, *118*, 7177.
[19] Y. Cohen, L. Avram, L. Frish, *Angew. Chem. Int. Ed.* **2005**, *44*, 520; *Angew. Chem.* **2005**, *117*, 524.
[20] G. W. V. Cave, M. C. Ferrarelli, J. L. Atwood, *Chem. Commun.* **2005**, 2787.
[21] S. J. Dalgarno, J. Antesberger, R. M. McKinlay, J. L. Atwood, *Chem. Eur. J.* **2007**, *13*, 8248.
[22] C. Zhang, R. S. Patil, T. Li, C. L. Barnes, J. L. Atwood, *Chem. Commun.* **2017**, *53*, 4312.
[23] R. S. Patil, H. Kumari, C. L. Barnes, J. L. Atwood, *Chem. Eur. J.* **2015**, *21*, 10431.
[24] R. S. Patil, A. M. Drachnik, H. Kumari, C. L. Barnes, C. A. Deakyne, J. L. Atwood, *Cryst. Growth Des.* **2015**, *15*, 2781.
[25] L. R. MacGillivray, J. L. Reid, J. A. Ripmeester, *Chem. Commun.* **2001**, 1034.
[26] L. R. MacGillivray, J. L. Atwood, *Supramol. Chem.* **2000**, *11*, 293.
[27] L. R. Macgillivray, K. T. Holman, J. L. Atwood, *Cryst. Eng.* **1998**, *1*, 87.
[28] G. W. Gokel, S. Negin, *Acc. Chem. Res.* **2013**, *46*, 2824.
[29] S. K. Menon, N. R. Modi, B. Mistry, K. Joshi, *J. Inclusion Phenom. Macrocyclic Chem.* **2011**, *70*, 121.
[30] E. K. Kazakova, N. A. Makarova, A. U. Ziganshina, L. A. Muslinkina, A. A. Muslinkin, W. D. Habicher, *Tetrahedron Lett.* **2000**, *41*, 10111.
[31] J. W. Steed, C. P. Johnson, C. L. Barnes, R. K. Juneja, J. L. Atwood, S. Reilly, R. L. Hollis, P. H. Smith, D. L. Clark, *J. Am. Chem. Soc.* **1995**, *117*, 11426.
[32] R. S. Patil, C. Zhang, J. L. Atwood, *Chem. Eur. J.* **2016**, *22*, 15202.
[33] B. C. Gibb, R. G. Chapman, J. C. Sherman, *J. Org. Chem.* **1996**, *61*, 1505.
[34] O. V. Kulikov, S. Negin, N. P. Rath, G. W. Gokel, *Supramol. Chem.* **2014**, *26*, 506.
[35] C. D. Gutsche, B. Dhawan, K. H. No, R. Muthukrishnan, *J. Am. Chem. Soc.* **1981**, *103*, 3782.
[36] L. M. Tunstad, J. A. Tucker, E. Dalcanale, J. Weiser, J. A. Bryant, J. C. Sherman, R. C. Helgeson, C. B. Knobler, D. J. Cram, *J. Org. Chem.* **1989**, *54*, 1305.
[37] L. Yasmin, T. Coyle, K. A. Stubbs, C. L. Raston, *Chem. Commun.* **2013**, *49*, 10932.

Manuscript received: November 25, 2017
Accepted manuscript online: December 31, 2017
Version of record online: February 8, 2018

© 2018 Wiley-VCH Verlag GmbH & Co. KGaA, Weinheim